Türk Doğa ve Fen Dergisi
Turkish Journal of Nature and Science
www.dergipark.gov.tr/tdfd

Determination of Gamma Radiation Shielding Characteristics for Some Iron-Based Metallic Glasses

Ferdi AKMAN[1*]

[1]Bingöl University, Vocational School of Social Sciences, Department of Property Protection and Security, Program of Occupational Health and Safety, 12000, Bingöl, Türkiye
Ferdi AKMAN ORCID No: 0000-0002-8838-1762

*Corresponding author: fakman@bingol.edu.tr

Abstract: In this study, the gamma radiation shielding characteristics of metallic glasses having Fe81B13.5Si3.5C2, Fe79B16Si5, Fe78B13Si9 and Fe40Ni38B18Mo4 components and coded as FeBSiC, FeBSi1, FeBSi2 and FeNiBMo were investigated. In order to investigate, the mass attenuation coefficients for metallic glasses in the photon energies range of 0.060 MeV to 2.614 MeV were calculated with the help of WinXCOM program and GEANT4 and FLUKA simulation codes. The linear attenuation coefficient, half and tenth value layers, mean free path, effective atomic number and electron density parameters were calculated with the help of the calculated mass attenuation coefficients. Variations of the calculated gamma radiation shielding parameters with photon energy were discussed. It was observed that mass and linear attenuation coefficients, effective atomic number and electron density parameters decreased with increasing photon energy, while half and tenth value layers and mean free path parameters increased with increasing photon energy. It has been observed that metallic glasses have better gamma shielding capabilities in the low photon energy region, and metallic glass coded as FeNiBMo has better gamma radiation shielding capacity than other studied metallic glasses.

Demir Tabanlı Bazı Metalik Camlar İçin Gama Radyasyonu Zırhlama Karakteristiklerinin Belirlenmesi

Öz: Sunulan bu çalışmada, Fe81B13.5Si3.5C2, Fe79B16Si5, Fe78B13Si9 ve Fe40Ni38B18Mo4 içeriklerine sahip ve FeBSiC, FeBSi1, FeBSi2 ve FeNiBMo olarak kodlanan metalik camların gama radyasyonu zırhlama karakteristikleri incelenmiştir. İnceleme yapmak için WinXCOM programı ve GEANT4 ve FLUKA simülasyon kodları yardımıyla 0.060 MeV ila 2.614 MeV foton enerjileri aralığında metalik camların kütle azaltma katsayıları hesaplanmıştır. Hesaplanan kütle azaltma katsayıları yardımıyla lineer azaltma katsayıları, yarı ve onda-bir kalınlık değerleri, ortalama serbest yol, etkin atom numarası ve elektron yoğunluğu parametreleri hesaplanmıştır. Hesaplanan gama radyasyonu zırhlama parametrelerinin foton enerjisi ile değişimleri irdelenmiştir. Kütle ve lineer azaltma katsayıları, etkin atom numarası ve elektron yoğunluğu parametrelerinin artan foton enerjisi azaldığı gözlemlenirken, yarı ve onda-bir kalınlık değerleri ve ortalama serbest yol parametrelerinin artan foton enerjisi ile arttığı gözlemlenmiştir. Düşük foton enerjisi bölgesinde metalik camların daha iyi gama zırhlama kabiliyetlerine sahip olduğu ve FeNiBMo olarak kodlanan metalik camın incelenen diğer metalik camlara göre daha iyi gama radyasyonu zırhlama kapasitesinin olduğu gözlemlenmiştir.

1. INTRODUCTION

Glass generally has an amorphous, non-crystalline structure, produced from silica (SiO_2) and oxides of metals such as Al, Mg, Ca, K and Na. Rapid cooling of silicate and metallic oxides is provided to prevent crystallization in glasses. During this rapid cooling process, the atoms in the liquid cannot rearrange themselves into the regular periodic structure, that is, as a crystalline solid. On the other hand, the term metallic glass refers to an amorphous metallic alloy prepared by rapid solidification of the molten metallic alloy. Metallic glasses are used in electricity and

electronics because of their high electrical resistance, in nuclear reactor engineering for the preparation of magnets in nuclear waste disposal containers and fusion reactors because their magnetic properties do not change under radiation, and in the biomedical industry because they can be used as cutting, making and prosthetic materials of surgical instruments due to their high resistance to corrosion. In addition, iron (Fe) and cobalt (Co) based metallic glasses generally show ferromagnetic properties.

Today, radiation is used to benefit humanity in medicine, industry, academic studies and electricity generation. In addition, radiation has useful applications in many fields such as agriculture, space exploration, geology and archaeology. Ionizing radiation exposure causes chemical damage to body tissues. Just as with exposure to any toxic chemical, the human body can tolerate radiation up to a point without causing any injury. However, high levels of exposure can cause serious problems such as skin burns, hair loss, internal bleeding, anemia and immune system involvement. Even very high exposure increases the risk of cancer.

The guiding principle for radiation protection is the ALARA "As Low As Reasonably Achievable" concept. The three main principles that will help this concept for radiation protection are time, distance and shielding. There is a linear relationship between the time spent near a radioactive source and the exposed radiation dose. The greater distance between the radiation source and the living thing, the less dose will be exposed. So, exposure is inversely proportional to the square of the distance. When the distance from the source is doubled, the exposure level will be four times less. In these two principles, exposure to radiation is seen as inevitable. In shielding, radiation exposure can be kept to a minimum. Today, lead aprons, mobile lead shields, lead glasses or lead barriers are generally preferred for protection from ionizing radiation. Due to the known toxic effects of lead and some problems arising from its weight, the search for new radiation shielding materials as an alternative to lead has gained momentum. Glasses [1-3], alloys [4-6], concretes [7-9], composites [10-12] and minerals [13,14] are included in the search new alternative products to lead. In addition to these, the choice of metallic glasses is a new alternative for use in this field, as their elements are adjustable up to a certain point.

Olarinoye and Oche [15] determined some radiation shielding parameters using XCOM and auto-Zeff programs in the energy range of 15 keV to 15 MeV to investigate the radiation shielding properties of titanium-based two metallic glasses. As a result of the calculations, they suggested that metallic glasses $Ti_{32.8}Zr_{30.2}Ni_{5.3}Cu_9Be_{22.7}$ and $Ti_{31.9}Zr_{33.4}Fe_4Cu_{8.7}Be_{22}$ could be good radiation shielding materials. Tekin et al. [16] investigated the radiation shielding capacities of metallic glasses having eight different concentrations in Cu_xZr_{100-x} (x=35 ($Cu_{35}Zr_{65}$)-70($Cu_{70}Zr_{30}$)) combination using MCNPX simulation

and Phy-X/PSD interface. For this purpose, they calculated the linear and mass attenuation coefficients, half value layer, tenth value layer, mean free path, effective atomic number and electron density parameters in the energy range of 0.015 to 15 MeV. They reported that $Cu_{70}Zr_{30}$ metallic glass is a better radiation shielding material than others. Perişanoğlu [17] investigated the alpha, proton, neutron and gamma radiation shielding capabilities of $Zr_{65}Al_{7.5}Ni_{10}Cu_{17.5}$, $Ti_{40}Zr_{26}Be_{28}Fe_6$, $Cu_{49}Hf_{42}Al_9$, $Pd_{40}Ni_{40}P_{20}$, $Ni_{50}Pd_{30}P_{20}$ and $Ca_{65}Mg_{15}Zn_{20}$ metallic glasses. He noted that among the studied metallic glasses, the $Cu_{49}Hf_{42}Al_9$ sample had better alpha, proton, neutron and gamma-ray shielding ability than the others. Tamam et al. [18] investigated the effect of Cu on gamma, charged particle and neutron shielding in metallic glasses with xCu-(20-x)Ge-40Se-40Te (0<x≤20) structure with the help of FLUKA simulation. They noted that 20% Cu-doped metallic glass shielded gamma, charged particles and neutrons better than the others. As can be seen from the literature review, the examination of the radiation shielding capabilities of metallic glasses is a very current issue and there are few studies on such samples.

There are two classes of metallic glasses as metal-metal and metal-metalloid. In the present study, Fe81B13.5Si3.5C2, Fe79B16Si5, Fe78B13Si9 and Fe40Ni38B18Mo4 metallic glasses belonging to the metal-metalloid class were preferred. In this study, Fe, Ni and Mo are metallic, while B, Si and C are metalloids. Gamma radiation shielding capabilities of the specified metallic glasses at energies (in the range of 0.060-2.614 MeV, 18 different energies) emitted from the most preferred radioactive sources in the literature were investigated with the help WinXCOM program [19], GEANT4 [20] and FLUKA [21] simulation codes. To compare the gamma radiation shielding capabilities of the specified metallic glasses, the mass and linear attenuation coefficients, half and tenth value layers, mean free paths, effective atomic numbers and electron densities were calculated.

2. MATERIAL AND METHODS

The gamma radiation shielding capacities of the specified metal-metalloid metallic glasses were investigated with the help of WinXCOM program, GEANT4 and FLUKA simulation codes. In order to estimate shielding performance, the chemical contents and densities of the metallic glasses presented in Table 1 were used.

Table 1. Codes, chemical compositions and densities of metallic glasses

Sample Code	Chemical Composition (%)						Density (g cm^{-3})
	Fe	B	Si	C	Ni	Mo	
FeBSiC [22]	81.0	13.5	3.5	2.0	-	-	7.32
FeBSi1 [23]	79.0	16.0	5.0	-	-	-	7.28
FeBSi2 [24]	78.0	13.0	9.0	-	-	-	7.18
FeNiBMo [25]	40.0	18.0	-	-	38.0	4.0	7.90

54

XCOM [26] is an online platform that gives partial cross-sections such as photoelectric, Compton scattering, pair production, triple production as well as attenuation coefficients of the elements, compounds or mixtures in the photon energy range from 1 keV to 100 GeV. WinXCOM is a Windows version of XCOM. GEANT4 is a code that simulates the passage of particles or photons through matter. With this code, operations such as geometry manipulation, tracking, run management and visualization can also be done. This code, which is generally used in high energy physics, is also preferred in space exploration, medical applications where radiation interactions are simulated, investigating radiation effects in semiconductors and nuclear physics. FLUKA is a code that simulates the interaction and propagation of sixty different particles, such as photons, electrons, neutrinos with matter in the energy range for 1 keV to thousands of TeV. FLUKA has usage areas such as radiation shielding studies, cosmic rays, neutrinos, detector design and dosimetry. In the presented paper, studies were carried out at photon energies of 0.060, 0.081, 0.088, 0.122, 0.136, 0.239, 0.356, 0.511, 0.569, 0.583, 0.662, 0.835, 1.063, 1.173, 1.275, 1.333, 1.770 and 2.614 MeV emitted from ^{22}Na, ^{54}Mn, ^{57}Co, ^{60}Co, ^{109}Cd, ^{133}Ba, ^{137}Cs, ^{207}Bi, ^{228}Th and ^{241}Am radioactive sources that are frequently used in the literature, industry, medicine and research laboratories. In the simulation codes, the interactions that can occur when ten million photons are radiated on the material are simulated. Detailed information about the simulation process has been reported in previous studies [27-28].

The mass attenuation coefficients of materials containing more than one element such as alloy, mineral, compound can be determined theoretically by the mixture rule method. In this method, the weight fraction of each element in the material and the mass attenuation coefficient of that element are multiplied to determine the contribution of the materials' total mass attenuation coefficient. After determining these additives for each element, they are summed to determine the mass attenuation coefficient of the material. The mixing rule is mathematically expressed in the equation below.

$$\left(\mu/\rho\right)_{material} = \sum_i W_i\left(\mu/\rho\right)_i \tag{1}$$

Here, W_i and $(\mu/\rho)_i$ are weight fraction and the mass reduction coefficient of the ith element. The weight fraction of elements in a material can be determined using the following equation.

$$W_i = \frac{n_i A_i}{\sum_j n_j A_j} \tag{2}$$

In the equation, n_i and A_i express the element number and atomic weight of the ith element in the material. The mass attenuation coefficient is a parameter independent of the density and phase state of the material. The linear attenuation coefficient is a parameter that changes with the density and phase state of the material and can be calculated from the mathematical multiply of the mass attenuation coefficient and the density of the material.

With the help of linear attenuation coefficient, half value layer (HVL), tenth value layer (TVL) and mean free path (MFP) parameters can be determined. They are defined as the material thickness that passes 50%, 10% and 36.8% of the initial radiation intensity, respectively, and these parameters can be determined with the help of the below equations.

$$HVL = \frac{ln2}{\mu} = \frac{0.693}{\mu} \tag{3}$$

$$TVL = \frac{ln10}{\mu} = \frac{2.303}{\mu} \tag{4}$$

$$MFP = \frac{1}{\mu} \tag{5}$$

The molecular, atomic and electronic cross-sections can be determined with the help of the mass attenuation coefficient. The molecular cross-section is determined by the following equation.

$$\sigma_{t,m} = \frac{1}{N}\left(\mu/\rho_{mater}\right)\sum_i (n_i A_i) \tag{6}$$

Here, N, $(\mu/\rho)_{mater}$, n_i and A_i are the Avogadro number, the total mass attenuation coefficient of the material, the element number and atomic weight of the ith element in the material, respectively. The relationship between the molecular cross-section and the atomic cross-section is shown in equation 7.

$$\sigma_{t,a} = \sigma_{t,m}/\sum_i n_i \tag{7}$$

The electronic cross-section could be obtained using equation 8.

$$\sigma_{t,e} = \frac{1}{N}\sum_i \frac{f_i A_i}{Z_i}\left(\mu/\rho\right)_i \tag{8}$$

Here, f_i, $(\mu/\rho)_i$ and Z_i express the abundance fraction, mass attenuation coefficient and atomic number of the ith element in the material, respectively. The effective atomic number is a parameter that can be obtained by dividing the atomic cross-section with electronic cross-section, and its mathematical representation is presented below.

$$Z_{eff} = \frac{\sigma_{t,a}}{\sigma_{t,e}} \tag{9}$$

Finally, the effective electron density can be

determined with the help of the equation 10.

$$N_E = \frac{Z_{eff}}{A_{tot}}(Nn_{tot}) \qquad (10)$$

Here, A_{tot} ve n_{tot} are the total atomic weight and number of elements in the material, respectively.

3. RESULTS AND DUSCUSSION

In the present study, gamma radiation shielding parameters of metallic glasses, whose codes, chemical components and densities are given in Table 1, were investigated in the photon energy range of 0.060 MeV to 2.614 MeV using WinXCOM program, GEANT4 and FLUKA simulation codes.

On this purpose, first of all, the mass attenuation coefficients of metallic glasses were determined by using the specified program and simulation codes. In Figure 1, the variation of the mass attenuation coefficients of the investigated metallic glasses according to the photon energy is presented, and in Table 2 the results of the mass attenuation coefficients of WinXCOM, GEANT4 and FLUKA are listed. When Figure 1 and Table 2 are examined, it is seen that the mass attenuation coefficients decrease exponentially with increasing photon energy and this parameter varies according to the elements in the metallic glasses. As seen in Figure 1, while the mass attenuation coefficients show a sharp decrease in the low energy region, this decrease is lower in the medium and high energy region. The reductions in these energy regions can be explained by the interaction events of the photon with matter. The dominant interaction process in the low energy region is the photoelectric event, while the dominant processes in the medium and high energy regions are Compton scattering and pair production events, respectively. Photoelectric cross-section depends on photon energy and atomic number as $E^{-3.5}$ and Z^{4-5}, respectively. While the relationship between Compton scattering cross-section between energy and atomic number is E^{-1} and Z, these dependencies are E and Z^2 for the pair production cross-section. Considering these proportionalities, the exponential decrease in the change of the mass attenuation coefficients with the photon energy is better understood. As can be seen in Figure 1 and Table 2, coded as FeNiBMo metallic glass containing nickel and molybdenum instead of low iron ratio has higher mass attenuation coefficients, especially in the low energy region. Therefore, this metallic glass has better gamma radiation shielding than other studied metallic glasses.

The linear attenuation coefficient, which is determined by the mass attenuation coefficient and the density of the material, is a more important gamma radiation shielding parameter in terms of usability. The graph of the linear attenuation coefficients depending on the photon energy for the investigated metallic glasses is shown in Figure 2.

Table 2. The mass attenuation coefficient results of WinXCOM, GEANT4 and FLUKA (cm^2 g^{-1}) for metallic glasses

Energy (MeV)	FeBSiC			FeBSi1			FeBSi1			FeNiBMo		
	WinX.	GEANT4	FLUKA	WinX.	GEANT4	FLUKA	WinX.	GEANT4	FLUKA	WinX.	GEANT4	FLUKA
0.060	1.012	0.929	1.150	0.993	0.911	0.995	0.989	0.907	0.991	1.256	1.159	1.545
0.081	0.499	0.452	0.556	0.492	0.445	0.492	0.490	0.443	0.490	0.603	0.550	0.720
0.088	0.420	0.380	0.464	0.414	0.374	0.414	0.413	0.373	0.413	0.502	0.456	0.594
0.122	0.239	0.216	0.256	0.236	0.214	0.237	0.236	0.214	0.236	0.271	0.246	0.307
0.136	0.206	0.187	0.219	0.204	0.186	0.205	0.204	0.186	0.204	0.230	0.209	0.256
0.239	0.124	0.117	0.126	0.123	0.117	0.123	0.124	0.117	0.124	0.129	0.122	0.149
0.356	0.099	0.096	0.100	0.099	0.096	0.099	0.099	0.096	0.099	0.101	0.098	0.103
0.511	0.083	0.082	0.083	0.083	0.082	0.083	0.083	0.082	0.083	0.084	0.083	0.090
0.569	0.079	0.078	0.079	0.079	0.078	0.079	0.079	0.078	0.079	0.080	0.079	0.082
0.583	0.078	0.077	0.079	0.078	0.077	0.078	0.078	0.077	0.078	0.079	0.078	0.082
0.662	0.073	0.073	0.073	0.073	0.073	0.073	0.074	0.073	0.074	0.074	0.074	0.076
0.835	0.066	0.066	0.066	0.066	0.066	0.066	0.066	0.066	0.076	0.066	0.066	0.069
1.063	0.058	0.058	0.058	0.058	0.058	0.058	0.058	0.058	0.058	0.058	0.058	0.059
1.173	0.055	0.055	0.055	0.055	0.055	0.055	0.055	0.055	0.055	0.056	0.056	0.056
1.275	0.053	0.053	0.053	0.053	0.053	0.053	0.053	0.053	0.053	0.053	0.053	0.054
1.333	0.052	0.052	0.052	0.052	0.052	0.052	0.052	0.052	0.052	0.052	0.052	0.052
1.770	0.045	0.045	0.045	0.045	0.045	0.045	0.045	0.045	0.045	0.045	0.045	0.046
2.614	0.038	0.038	0.038	0.038	0.038	0.038	0.038	0.038	0.038	0.038	0.038	0.038

Figure 1. Variation of mass attenuation coefficients with photon energy for the studied metallic glasses

As can be seen in Figure 2, the variation of linear attenuation coefficients with energy shows a similar trend as the variation of mass attenuation coefficients with energy. That is, the linear attenuation coefficients decrease exponentially with increasing photon energy. At 0.060 MeV, linear attenuation coefficients of FeBSiC, FeBSi1, FeBSi2 and FeNiBMo metallic glasses are 7.4086, 7.2310, 7.1031 and 9.9196 cm^{-1}, respectively, while these values are 0.5372, 0.5338, 0.5280 and 0.5842 cm^{-1} at 0.662 MeV, respectively. It is seen that the difference between the linear attenuation coefficients decreases as the photon energy increases. This can be explained by photon-matter interaction processes as interpreted by the mass attenuation coefficients in the low, medium and high energy regions. While the investigated metallic glasses show good gamma radiation shielding properties in the low energy region, coded as FeNiBMo metallic glass with high linear attenuation coefficients and density has higher gamma radiation shielding capacity than the others.

Other parameters that are important for material usability are half and tenth value layers and mean free path. The variation of these parameters with photon energy is shown in Figures 3-5, respectively. As can be

seen from Equation 3-5, these parameters are inversely proportional to the linear attenuation coefficient and these parameters are important parameters as they indicate the absorber thickness required to reduce certain amounts of radiation intensity.
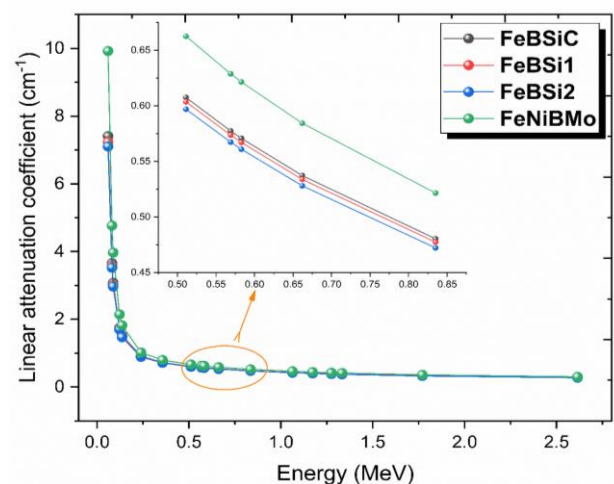
Figure 2. Variation of linear attenuation coefficients with photon energy for the studied metallic glasses

It can be seen from Figures 3-5 that these parameters increase with increasing photon energy since they are

inversely proportional to the linear attenuation coefficient. At 0.060 MeV, the half value layers of FeBSiC, FeBSi1, FeBSi2 and FeNiBMo metallic glasses are 0.0936, 0.0959, 0.0976 and 0.0699 cm, respectively, according to WinXCOM results, while these values are 1.2902, 1.2985, 1.3127 and 1.1864 cm, respectively at 0.662 MeV. So, in order to reduce half of the incident radiation intensity at photon energies of 0.060 and 0.662 MeV, the investigated metallic glasses must have the above-mentioned thicknesses. When the half value layers at the mentioned energies above and Figures 3-5 are examined, coded as FeNiBMo metallic glass has lower half and tenth value layers and mean free path values. Therefore, this metallic glass is a better gamma radiation shielding material than others.
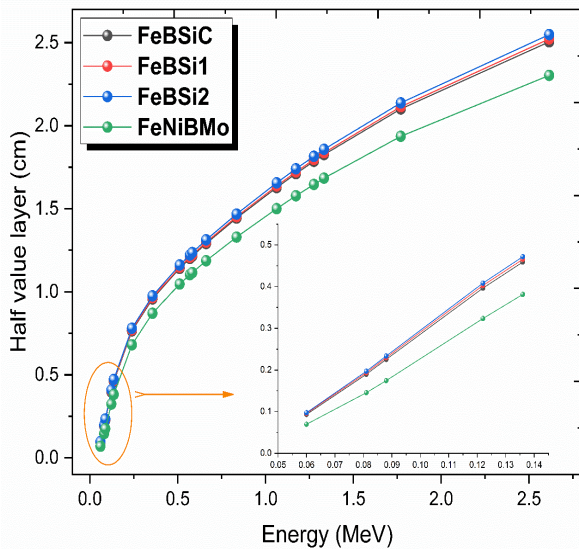
Figure 3. Variation of half value layers with photon energy for the studied metallic glasses
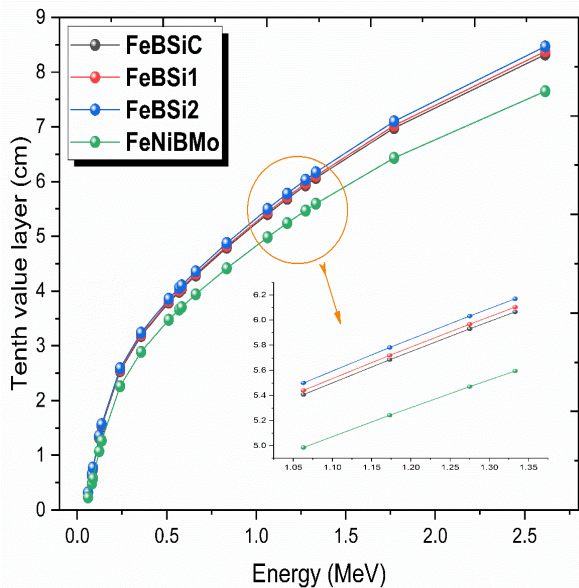
Figure 4. Variation of tenth value layers with photon energy for the studied metallic glasses
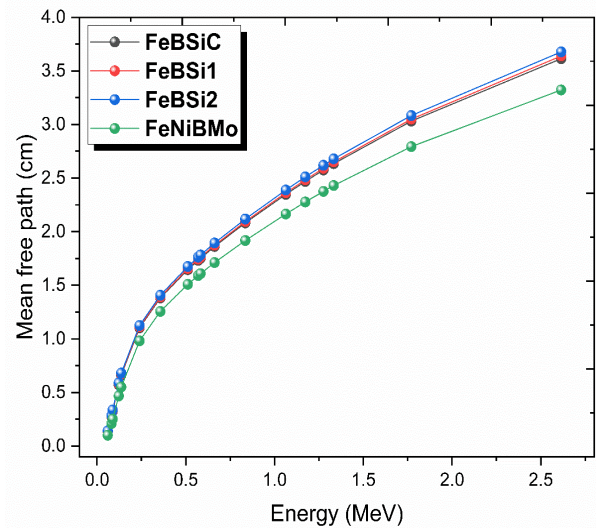
Figure 5. Variation of mean free path with photon energy for the studied metallic glasses

The determined another parameter using the mass attenuation coefficient is the effective atomic number. The large values of the effective atomic number indicate that the material is a good gamma radiation shielding material. The variation of the effective atomic numbers with the photon energy for the investigated metallic glasses is seen in Figure 6. As seen from the figure, the effective atomic numbers of metallic glasses are listed as FeNiBMo>FeBSiC>FeBSi2>FeBSi1. Also, as seen in Figure 6, the effective atomic number decreases exponentially with photon energy. Changes in different energy regions can be interpreted according to photoelectric, Compton scattering and pair production cross-sections, as explained in other parameters.

58
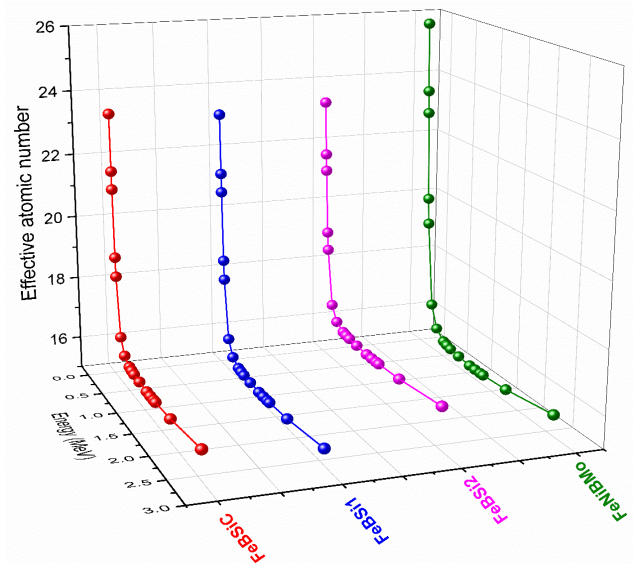
Figure 6. Variation of effective atomic number with photon energy for the studied metallic glasses

The effective electron density is a parameter related to the effective atomic number and their variation with photon energy is presented in Figure 7. According to

this figure, the effective electron densities are listed as FeNiBMo>FeBSiC>FeBSi1>FeBSi2. When Equation 10 is examined, there is a direct proportionality between the effective atomic number and the effective electron density. So, as the effective atomic number increases, the effective electron density also increases, or vice versa. This proportionality can be seen in Figure 8. However, the effective electron density is directly proportional to the total number of atoms in the material and inversely proportional to the sum of the atomic weights of the elements in the material, except for the effective atomic number. The effective atomic number of FeBSi2 sample is greater than that of FeBSi1 sample, but the effective electron density of FeBSi2 is smaller than that of FeBSi1. This difference is due to the number or atomic weights of the elements in the metallic glass. When the figures for effective number and electron density are examined, FeNiBMo metallic glass has better gamma radiation shielding than other metallic glasses.
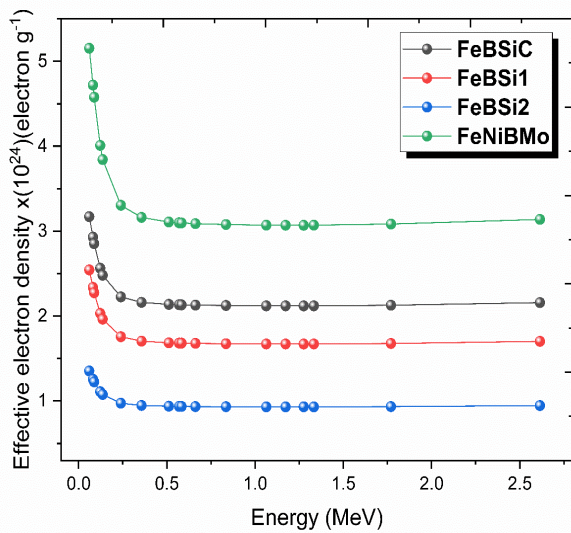
Figure 7. Variation of effective electron density with photon energy for the studied metallic glasses
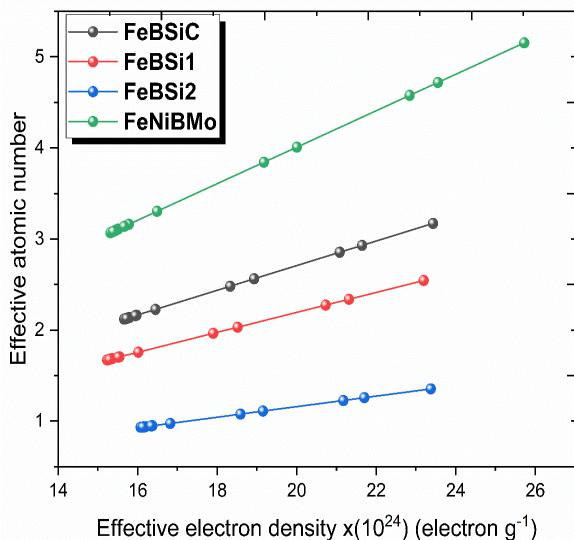
Figure 8. Variation of effective atomic number with effective electron density

4. CONCLUSIONS

In the present study, the gamma radiation shielding capacities of Fe81B13.5Si3.5C2, Fe79B16Si5, Fe78B13Si9 and Fe40Ni38B18Mo4 metallic glasses were investigated in the photon energies range of 0.060 to 2.614 MeV (18 different energies). For this, WinXCOM program, GEANT4 and FLUKA simulation codes are used. It was observed that mass and linear attenuation coefficients, effective atomic number and electron density parameters decreased with increasing photon energy, while half and tenth value layers and mean free path parameters increased with increasing photon energy for the investigated metallic glasses. When all the calculated gamma radiation shielding parameters were examined, it was observed that all metallic glasses had good gamma radiation shielding characteristics in the low energy region, and metallic glass coded as FeNiBMo had better gamma shielding capacity than other metallic glasses. The investigated metallic glasses can be used in electrical and electronics, nuclear waste disposal containers, nuclear reactors in terms of shielding gamma radiation, as well as radiation-related units of hospitals, space research and laboratories where radiation studies are carried out.

REFERENCES

[1] Halimah MK, Azuraida A, Ishak M, Hasnimulyati L. Influence of bismuth oxide on gamma radiation shielding properties of boro-tellurite glass. J Non-cryst Solids. 2019; 512: 140-7.

[2] Al-Buriahi MS, Sriwunkum C, Arslan H, Tonguc BT, Bourham MA. Investigation of barium borate glasses for radiation shielding applications. Appl Phys A-Mater. 2020; 126(1): 1-9.

[3] El-Sharkawy RM, Shaaban KS, Elsaman R, Allam EA, El-Taher A, Mahmoud ME. Investigation of mechanical and radiation shielding characteristics of novel glass systems with the composition xNiO-20ZnO-60B2O3-(20-x) CdO based on nanometal oxides. J Non-cryst Solids. 2020; 528: 119754.

[4] Kaur T, Vermani YK, Al-Buriahi MS, Alzahrani JS, Singh T. Comprehensive investigations on radiation shielding efficacy of bulk and nano Pb-Sn-Cd-Zn alloys. Phys Scripta. 2022; 97(5): 055009.

[5] Turhan MF, Akman F, Taşer A, Dilsiz K, Oğul H, Kacal MR, et al. Gamma radiation shielding performance of CuxAg (1-x)-alloys: Experimental, theoretical and simulation results. Prog Nucl Energ. 2022; 143: 104036.

[6] Alzahrani JS, Alrowaili ZA, Eke C, Mahmoud ZM, Mutuwong C, Al-Buriahi MS. Nuclear shielding properties of Ni-, Fe-, Pb-, and W-based alloys. Radiat Phys Chem. 2022; 195: 110090.

[7] Zeyad AM, Hakeem IY, Amin M, Tayeh BA, Agwa IS. Effect of aggregate and fibre types on ultra-high-performance concrete designed for radiation shielding. J Build Eng. 2022; 58: 104960.

Tr. Doğa ve Fen Derg. Cilt 12, Sayı 1, Sayfa 53-60, 2023

Tr. J. Nature Sci. Volume 12, Issue 1, Page 53-60, 2023

[8] Kharita MH, Takeyeddin M, Alnassar M, Yousef S. Development of special radiation shielding concretes using natural local materials and evaluation of their shielding characteristics. Prog Nucl Energ. 2008; 50(1): 33-6.

[9] Makarious AS, Bashter II, Abdo AES, Azim MSA, Kansouh WA. On the utilization of heavy concrete for radiation shielding. Ann Nucl Energy. 1996; 23(3): 195-206.

[10] Cherkashina NI, Pavlenko VI, Noskov AV. Radiation shielding properties of polyimide composite materials. Radiat Phys Chem. 2019; 159: 111-7.

[11] Saleh HM, Bondouk II, Salama E, Esawii HA. Consistency and shielding efficiency of cement-bitumen composite for use as gamma-radiation shielding material. Prog Nucl Energ. 2021; 137: 103764.

[12] Okafor CE, Okonkwo UC, Okokpujie IP. Trends in reinforced composite design for ionizing radiation shielding applications: a review. J Mat Sci. 2021; 56(20): 11631-55.

[13] Özdemir HG, Demirkol İ, Erkoyuncu İ, Yılmaz M, Kaçal MR, Akman F. Bazı Tungsten İçerikli Minerallerin Gama Zırhlama Özelliklerinin Geniş Enerji Aralığında İncelenmesi. J Inst Sci Tech. 2022; 12(4): 2175-87.

[14] Turhan MF, Akman F, Kaçal MR, Durak R. Calculation of Absorption Parameters for Some Selected Minerals in the Energy Range of 1 keV to 100 GeV. Int J Sci Eng Res. 2019; 10(9): 56-61.

[15] Olarinoye O, Oche C. Gamma-ray and fast neutron shielding parameters of two new titanium-based bulk metallic glasses. Iran J Med Phys. 2021; 18(2): 139-147.

[16] Tekin HO, ALMisned G, Susoy G, Zakaly HM, Issa SA, Kilic G, et al. A detailed investigation on highly dense CuZr bulk metallic glasses for shielding purposes. Open Chem. 2022; 20(1): 69-80.

[17] Perişanoğlu U. Assessment of nuclear shielding and alpha/proton mass stopping power properties of various metallic glasses. Appl Phys A-Mater. 2019; 125(11): 1-11.

[18] Tamam N, Alrowaili ZA, Elqahtani ZM, Somaily HH, Alwadai N, Sriwunkum C, et al. Significant influence of Cu content on the radiation shielding properties of Ge-Se-Te bulk glasses. Radiat Phys Chem. 2022; 193: 109981.

[19] Gerward L, Guilbert N, Jensen KB, Levring H. WinXCom—a program for calculating X-ray attenuation coefficients. Radiat Phys Chem. 2004; 71(3-4): 653-4.

[20] Agostinelli S, Allison J, Araujo H, Arce P, Asai M, Axen D, et al. GEANT4-a simulation toolkit. Nucl Instrum Meth A. 2003; 506 (3): 250-303.

[21] Böhlen TT, Cerutti F, Chin MPW, Fassò A, Ferrari A, Ortega PG, et al. The FLUKA code: developments and challenges for high energy and medical applications. Nucl Data Sheets. 2014; 120: 211-4.

[22] Goodfellow [Internet]. [cited 2023 Feb 05] Available from: https://www.goodfellow.com/uk/en-gb/displayitemdetails/p/fe80-fl-000150/iron-boron-silicon-foil

[23] Goodfellow [Internet]. [cited 2023 Feb 05] Available from: https://www.goodfellow.com/uk/en-gb/displayitemdetails/p/fe82-fl-000150/iron-boron-silicon-foil

[24] Goodfellow [Internet]. [cited 2023 Feb 05] Available from: https://www.goodfellow.com/uk/en-gb/displayitemdetails/p/fe81-fl-000150/iron-boron-silicon-foil

[25] Goodfellow [Internet]. [cited 2023 Feb 05] Available from: https://www.goodfellow.com/uk/en-gb/displayitemdetails/p/fe83-fl-000150/iron-nickel-boron-foil

[26] Gerward L, Guilbert N, Jensen KB, Levring H. X-ray absorption in matter. Reengineering XCOM. Radiat Phys Chem. 2011; 60(1-2): 23-4.

[27] Kilicoglu, O, Akman F, Oğul H, Agar O, Kara U. Nuclear radiation shielding performance of borosilicate glasses: Numerical simulations and theoretical analyses. Radiat Phys Chem. 2023; 204: 110676.

[28] Ozdogan, H, Kilicoglu O, Akman F, Agar O. Comparison of Monte Carlo simulations and theoretical calculations of nuclear shielding characteristics of various borate glasses including Bi, V, Fe, and Cd. Appl Radiat Isotopes. 2022; 189: 110454.